Chapter 11

Bis-pyridylethenyl benzene as novel backbone for amyloid-β binding compounds

Submitted

Rob J.A. Nabuurs[1]
Varsha V. Kapoerchan[2]
Athanasios Metaxas[3]
Sarah Hafith[1]
Maaike de Backer[1]
Mick M. Welling[1]
Wim Jiskoot[4]
Adrianus M.C.H. van den Nieuwendijk[2]
Albert D. Windhorst[3]
Herman S. Overkleeft[2]
Mark A. van Buchem[1]
Mark Overhand[2]
Louise van der Weerd[1,5]

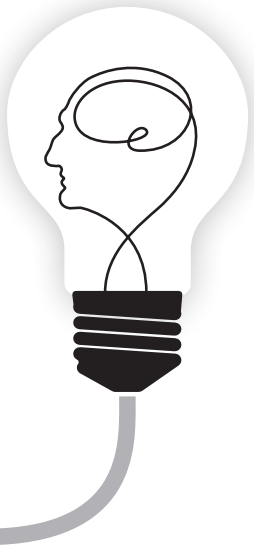

Abstract

Detection of cerebral β-amyloid (Aβ) by targeted contrast agents is of great interest for *in vivo* diagnosis of Alzheimer's disease (AD). Partly because of their planar structure several bis-styrylbenzenes have been previously reported as potential Aβ imaging agents. However, these compounds are relatively hydrophobic, which likely limits their *in vivo* potential. Based on their structures, we hypothesized that less hydrophobic bis-pyridylethenylbenzenes may also label amyloid. We synthesized several bis-pyridylethenylbenzenes and tested whether these compounds indeed display improved solubility and lower LogP values, and studied their fluorescent properties and Aβ binding characteristics. Bis-pyridylethenylbenzenes showed a clear affinity for Aβ plaques on both human and murine AD brain sections. Competitive binding experiments suggested a different binding site than Chrysamine G, a well-known stain for amyloid. With a LogP value between 3 and 5, most bis-pyridylethenylbenzenes were able to enter the brain and label murine amyloid *in vivo* with overall the bis(4-pyridylethenyl)benzenes showing the most favorable characteristics. In conclusion, the presented results suggest that bis-pyridylethenylbenzene may serve as a novel backbone for amyloid imaging agents.

Introduction

Cerebral accumulation of senile amyloid plaques plays an important role in the pathogenesis of Alzheimer's disease (AD), as it is thought to precede the onset of the first clinical symptoms by up to two decades.[1,2] These typical deposits of fibrillar amyloid-β peptides (Aβ) thereby constitute an important target for the development of imaging agents capable of visualizing and quantifying them. Much progress has been made in the development of such Aβ-targeting imaging ligands suitable for visualization by positron emission tomography (PET), single positron emission tomography (SPECT), fluorescence microscopy or magnetic resonance imaging (MRI).

Pittsburgh compound B (PiB, **1**, **Figure 11.1**), a [^{11}C]-benzothiazole derivative, is the best characterized *in vivo* PET radiotracer thus far. The short half-life of ^{11}C however limits its use to medical centers with an on-site cyclotron. In addition longer-lived ^{18}F radiofluorinated derivatives have been synthesized, like flutemetamol (**2**)[3], florbetapir (**3**) and florbetaben(**4**)[4], of which the first two recently were approved by the U.S. Food and Drug Administration for commercial use.[5,6] However improved Aβ-targeted imaging agents or backbones that could potentially outperform previous agents, bind to specific subtypes of cerebral amyloid or that are suitable for other clinical imaging modalities are still warranted.

The precise mechanisms that cause these small molecules to bind specifically to amyloid structures are still not completely understood.[7] An hypdrophobic planarized π system is hypothesized as an important design feature for high binding specificity based on a well-known histological amyloid dye, Congo Red (**5**).[8] *In vivo* application of Congo Red however was not feasible due its limited brain entry. Its molecular structure served as backbone for the development of bis-styrylbenzene imaging probes for PET, SPECT and ^{19}F MRI, like **6** (Chrysamine G), **7** (X-34)[9], **8** (ISB)[10], **9** (FSB)[12]and **10** (Methoxy-X04)[11]. (**Figure 1**) The acidic functional groups appeared to be unnecessary for high affinity Aβ binding, while bis-styrylbenzenes lacking these groups showed K_d's ~300 fold lower compared to **9**.

Unfortunately, the use of amyloid targeting bis-styrylbenzenes is limited to preclinical imaging studies that exploit their fluorescent properties.[15] Despite the promising initial *in vivo* ^{19}F MRI performed with **9** the incorporation of multiple fluorine atoms thus far has not sufficiently increased their sensitivity for the use as an MRI contrast agent.[13,14] In general, many of these compounds are very hydrophobic, their poor aqueous solubility and blood-brain barrier (BBB) passage are likely to limit the *in vivo* imaging potential of these compounds or lead to an unfavorable cerebral washout that causes non-specific signal of unbound compound.

We envisioned that replacement of the phenyl outer rings of the (bis)styrylbenzene backbone with pyridine rings may overcome some of these hurdles, as the presence of the nitrogen atom is expected to improve solubility and lower LogP values. This study therefore aims to investigate whether bis-pyridylethenyl benzene may serve as a new backbone for the development of an amyloid-β targeting imaging agent. Synthesized compounds were evaluated with respect to their *in vitro* Aβ binding and specificity, and their fluorescent properties. Partition coefficients (LogP) were determined to assess hydrophobicity. *In vivo* affinity for amyloid plaques and cerebral entrance was evaluated following intravenous injection of the compound in a transgenic AD mouse model.

Design

We designed a series of six different bis-pyridylethenylbenzenes (**11 – 16**) with the amyloid-targeting compound Methoxy-X04 (**10**)[11] set as starting point for the design and synthesis. (**Figure 11.2**) With an affinity for Aβ plaques in the nanomolar range (K_i = 26.8 nM), this fluorescent small molecule is frequently used for intravital microscopy studies *in vivo* following intravenous or intraperitoneal injection.[11] Compounds **11 – 13** have no substituents at all and can serve to evaluate whether the presence of the two nitrogen atoms can compensate for the hydroxy- and methoxy functionalities in Methoxy-X04. Compounds **14 – 16** contain a methoxy-substituent on the middle ring for a more direct comparison with Methoxy-X04.

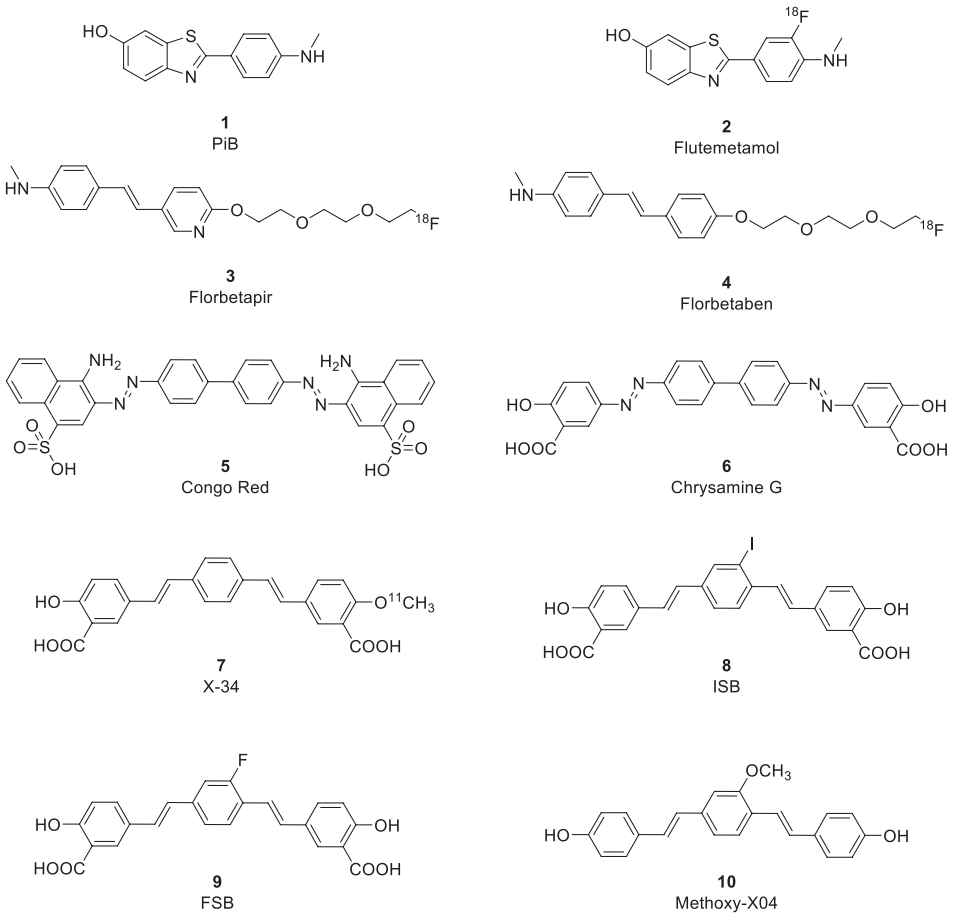

Figure 11.1 Previously reported amyloid-β binding ligands

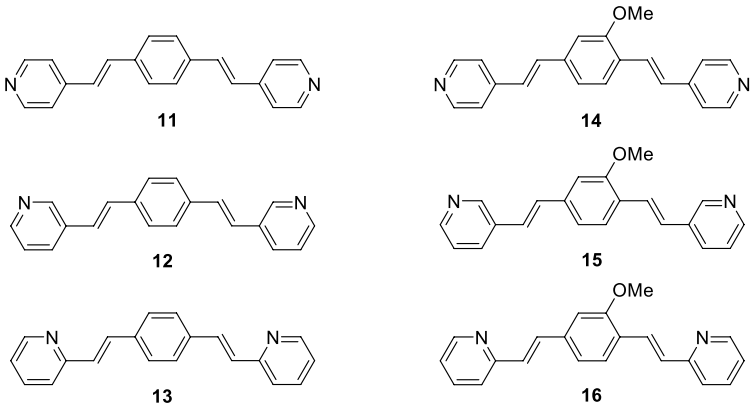

Figure 11.2 Envisioned bis-pyridylethenylbenzenes

All these compounds are accessable using the general synthesis route recently separately published by ourselves[14] and the group of Boländer *et al.*[16], which is depicted in **Scheme 11.1** with the key building blocks being diphosphonate **C** and an aldehyde **D**. p-xylene **A** is subjected to radical bromination to yield dibromide **B**. This dibromide is then treated with triethyl phosphite in an Arbuzov reaction to give diphosphonate **C**. A Horner-Wadsworth-Emmons reaction between diphosphonate **C** and an aldehyde **D** yields (E,E)-bis-pyridylethenylbenzene **E**.
The building blocks needed for the synthesis of compounds **11 – 16** are either easily synthesized or commercially available. (**Figure 11.3**) With all building blocks in hand, compounds **11 – 16** were synthesized. The synthesis proceeded uneventful, and all compounds were obtained in reasonable yields (14 – 45%).

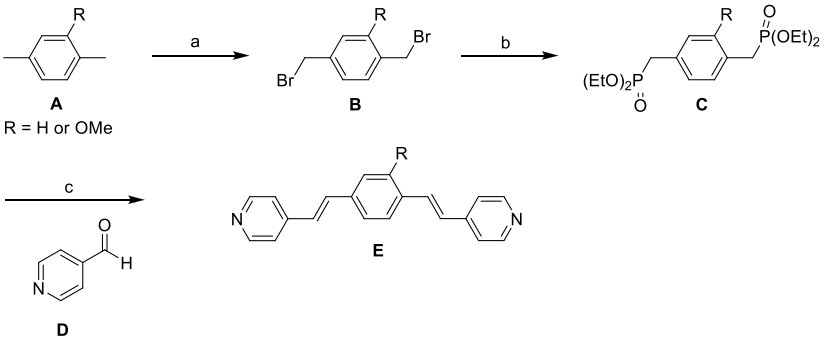

Scheme 11.1 General synthesis route for the envisioned bis-pyridylethenyl benzenes
Reagents and conditions: **a**) N-bromosuccinimide, benzoyl peroxide, CCl4, reflux, 16 h. **b**) Triethyl phosphite, 150 °C, 16 h. **c**) 1. KOtBu, THF, -10 °C, 20 min. then D, rt, 16 h.

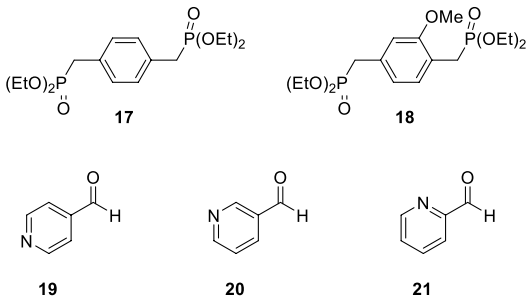

Figure 11.3 The required building blocks

Results and Discussion

Fluorescent properties

All synthesized compounds are expected to have fluorescent properties based on their conjugated ring structures. We therefore determined excitation and emission wavelength maxima of 300 nM solutions and the emission intensities were compared to that of Methoxy-X04. (**Table 11.1**) The intrinsic fluorescent intensity was typically higher for the bis(3-pyridylethenyl) benzenes compared to the bis(2-pyridylethenyl)benzenes.

It has been reported that binding to amyloid may have a significant effect on fluorescence properties[17], and therefore the fluorescence was also measured in the presence of synthetic Aβ fibrils. The parent compound **10** showed the highest fluorescence yield with a 10-fold increase in the presence of amyloid fibrils. All tested bis-pyridylethenylbenzenes showed an increase of fluorescence after binding, with compound 12 being the brightest. (**Table 11.1**) Several previously reported Aβ-targeting fluorophores have shown a clear red-shifted emission spectrum following binding[18,19], but such a spectral shift was not observed for any of the tested bis-pyridylethenylbenzenes.

Qualitative assessment of human and murine amyloid plaques binding

Fluorescence microscopy was used for a qualitative *ex vivo* assessment of the amyloid-binding properties. A concentration series of each compound (1 – 10 – 100 μM) was applied to brain sections of AD patients and of aged APPswe-PS1ΔE9 (APP/PS1) mice, which have a high amyloid plaque load. At 100 μM all compounds showed characteristic staining of amyloid plaques on murine APP-PS1 brain sections. Although all compounds bound to amyloid plaques at high concentration, differences in binding became visible at the lower concentrations. (**Table 11.1** and **Figure 11.4**) No non-specific background labeling or labeling of neurofibrillary tangles (NFTs) was observed at these concentrations suggesting their specificity for amyloid.

As stated in the previous paragraph, the fluorescence intensity with and without amyloid fibrils differed significantly for the various compounds. Therefore, the fluorescence intensity in the presence of fibrils was calculated and expressed relative to the intensity of Methoxy-X04 (**10**). (**Table 11.1**) Assuming that the fluorescence yield in the presence of synthetic Aβ is representative for that in the presence of amyloid plaques, the staining data was interpreted

Table 11.1 Fluorescent and binding characteristics

Compound	MW	λ_{ex}[a]	λ_{em}	Fluorescence intensity[b]	Fluoresence intensity on binding to fibrillar Aβ[b]	Fold increase on binding to fibrillar Aβ	*Ex vivo* Aβ binding[c]	
		(all ± 1nm)	(all ± 1nm)	(%)	(%)		Human	Murine
10	344.403	372	451	100	982	9.82	+	+
11	284.354	354	420	70	227	3.23	++	+++
12	284.354	352	412	225	505	2.24	+	++
13	284.354	356	415	57	312	5.48	++	+++
14	314.380	373	430	16	130	8.18	- -	+
15	314.380	360	436	185	359	1.94	- -	-
16	314.380	362	441	38	189	4.99	- -	+

[a] Ex/Em wavelength maxima were determined of 300 nM solutions. [b] Fluoresence intensity was calculated relative to that of 10. [c] Staining of amyloid plaques in human and APP-PS1 murine at 1 µM was scored whether the compound stained nothing (-), less (-), similar (+), slightly more (++) or much more (+++) for amyloid plaques in comparison to **10**.

as follows. With no substitution on the inner ring bis-pyridylethenylbenzenes **11 – 13** displayed improved amyloid labeling compared to Methoxy-X04 (**10**). This was already shown for a similar bis-styrylbenzene lacking additional groups, suggesting that planarity indeed plays an important role.[20] Although compounds **12** and **15** expressed the highest fluorescent intensity after synthetic amyloid binding of all tested bis-pyridylethenylbenzenes, their ability to depict amyloid plaques on brain sections seemed less clear. This would suggest that incorporation of a nitrogen atom on the 3rd position results in less favorable binding characteristics. Incorporation of an additional methoxy-group (**14** and **16**) resulted in a slightly reduced binding on the murine sections. Compared to Methoxy-X04, however, their ability to depict murine amyloid seems better, as the fluorescence yield of compounds **14** and **16** is lower. This suggests that the nitrogen alone might be sufficient to replace the hydroxy groups present in Methoxy-X04 (**10**). Similar to Methoxy-X04, the affinity of the ligands for human plaques appears to be less than for the murine plaques. As amyloid plaques in humans and mice differ in composition and compactness[21], this is likely the reason for the observed differences in staining between human and murine AD sections. Nevertheless, staining of human tissue could still be clearly observed for compounds **11 – 13**, and was improved compared to Methoxy-X04 for compound **11** and **13**.

Affinity for synthetic Amyloid-β fibrils

A competition assay with tritiated amyloid dye Chrysamine G (**6**) was used to determine the binding inhibition coefficient (Ki) for the compounds.[11] Unlike compound **10**, none of the bis-pyridylethenylbenzenes showed any competitive binding to [^{3}H]Chrysamine G using either synthetic amyloid fibrils (**Figure 11.5**) or

murine brain homogenate. (**Figure 11.6**) This implies that these compounds use a different binding site than Chrysamine G, and most likely Methoxy-X04 (**10**). Unfortunately, we were therefore unable to determine Ki values for the synthesized compounds.

LogP values

The blood-brain barrier (BBB) is formed by a tight layer of endothelial cells in the wall of cerebral blood vessels that regulates the exit and entry of blood compounds into the brain. It is traditionally stated that for optimal passive BBB passage, compounds should preferably have moderately hydrophobicity (LogD or LogP 2.0 - 3.5), although several successful radiopharmaceuticals do not meet this requirement.[22] Therefore LogD or LogP should be

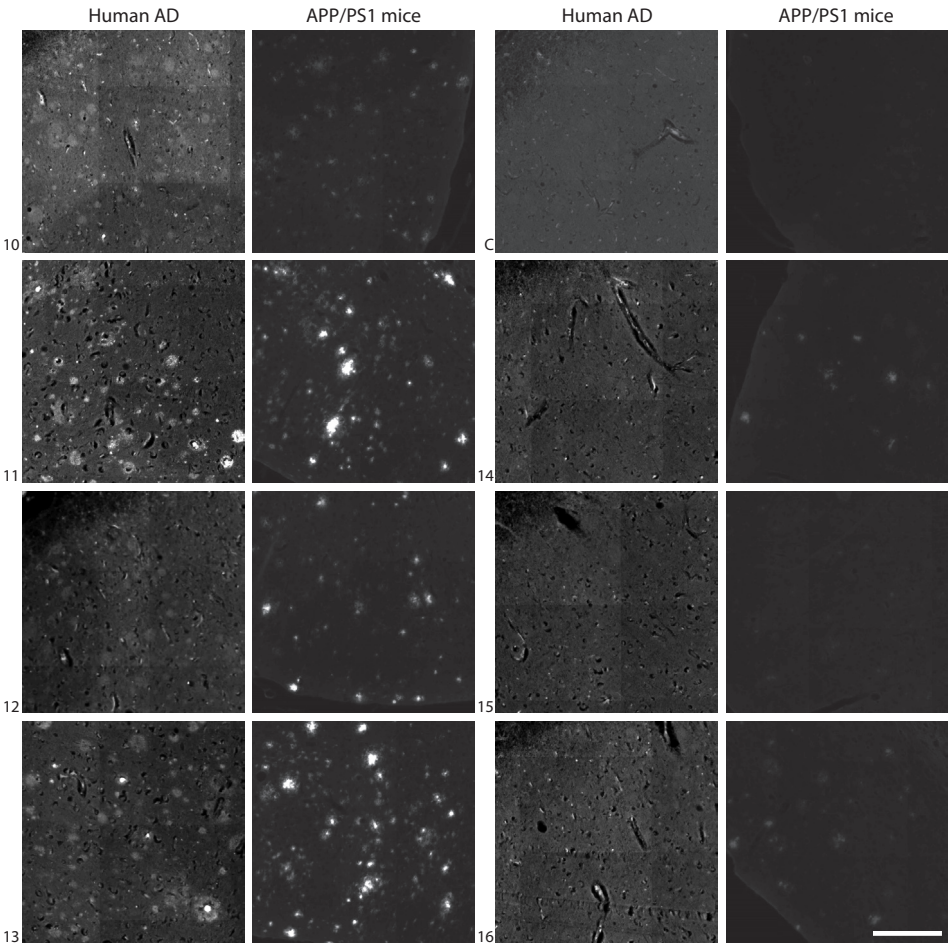

Figure 11.4 Staining of human and APP/PS1 murine amyloid plaques
All bis-pyridylethenylbenzenes stained both human and murine amyloid plaques after applying 100 µM (data not shown). At 1 µM concentration, differences in binding between the compounds become apparent compared to each other or the negative controls (**C**). All images were taken with the same microscope settings. Scale bar = 200 µm.

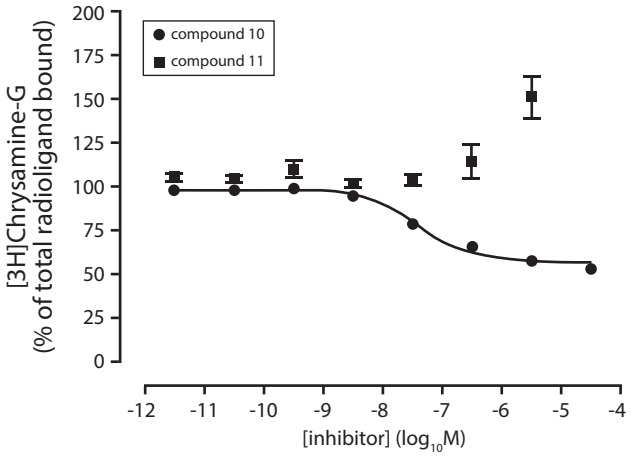

Figure 11.5 Competition binding with synthetic Aβ fibrils
Displacement of [^{3}H]ChrysamineG binding by Methoxy-X04 (**10**) (closed circles) and compound **11** (open circles), on fibrilized synthetic $A\beta_{1\text{-}40}$. Data are presented as the mean ± SEM of one experiment, conducted in triplicate, and replicated three to seven independent times. **10** inhibited the binding of 5 nM [^{3}H]Chrysamine G with a mean Ki value of 24.1 ± 8.0 nM.

carefully considered as selection criterion, but when it is applied within one series of compounds it is nonetheless a valid parameter for selection. For each of the compounds **10 – 16**, LogP values were determined with an HPLC-based method according to Benhaim *et al*.[23-25] All compounds have a LogP below that of Methoxy-X04, although none of them meets the before mentioned criterion. (**Table 11.2**)

In vivo amyloid plaque labeling in transgenic AD mice

To assess the ability of the compounds to pass the BBB *in vivo*, solutions of each compound were injected at 30 µmol/kg in aged transgenic APP/PS1 mice, which have extensive cerebral amyloid plaques. One day after injection the mice were sacrificed, their brains were removed and sections were studied according to the fluorescence microscopy set-up used for the stained brain sections. All compounds were readily dissolved using a mixture of 0.05 M compound dissolved in 1:1 DMSO:Cremophor (volume ratio) diluted up to 200 µl with PBS at pH 7.2. Disolving bis(2-pyridylethenyl)benzenes **13** and **16** however resulted in a viscous substance that was not well tolerated by the animals. *In vivo* targeting of amyloid plaque however was observed for all compounds, showing their ability to pass the BBB. (**Figure 11.7** and **Table 11.2**) No non-specific labeling was detected in the wild type brain. Direct comparison of the *in vivo* amyloid labeling between the different compounds remained difficult, as the amyloid load may differ between the transgenic animals and the fluorescence yield of the compounds varies considerably. Bis-pyridylethenylbenzene **11** showed a comparable signal intensity in individual labeled plaques after intravenous injection compared to Methoxy-X04, while having a 4-fold lower fluorescence yield. Also its methoxy variant, compound **14**, clearly crossed the BBB *in vivo* to label amyloid plaques despite of an almost 10-fold lower fluorescence yield after binding compared to Methoxy-X04.

Table 11.2 LogP values and *in vivo* amyloid labeling

compound	LogP (calc)a	LogP (determined)	In vivo amyloid labeling
10	5.55	4.84	+
11	3.94	3.93	+
12	3.94	3.73	+
13	4.12	3.75	+
14	3.86	3.73	+
15	4.03	4.32	+
16	4.16	4.25	+

[a]LogP values were calculated used web-based methods: www.molinspiration.com and http://intro.bio.umb.edu/111-112/OLLM/111F98/jLogP/test.html. The ability to label amyloid plaques in the brains of APP-PS1 mice following intravenous injection were scored absent (-) or present (+).

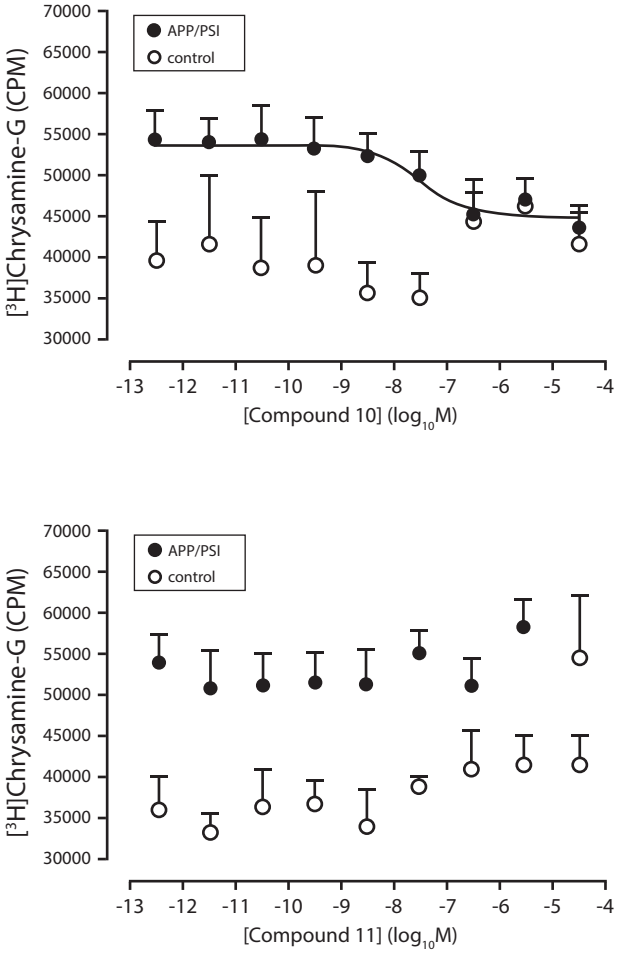

Figure 11.6 Binding competition with APP/PS1 transgenic brain homogenates

Displacement of [^{3}H]Chrysamine G binding by Methoxy-X04 (**10**) (**A**) and compound **11** (**B**), on brain cortex homogenates of 11 months-old APP/PS1 transgenic and control mice. Data are presented as the mean ± SEM of one experiment, conducted in duplicate and replicated three independent times. **10** inhibited the binding of 5 nM [^{3}H]Chrysamine G in APP/PS1 mice (closed circles) with a K_i value of 27.5 ± 3.5 nM, which is in good agreement with literature.[28]

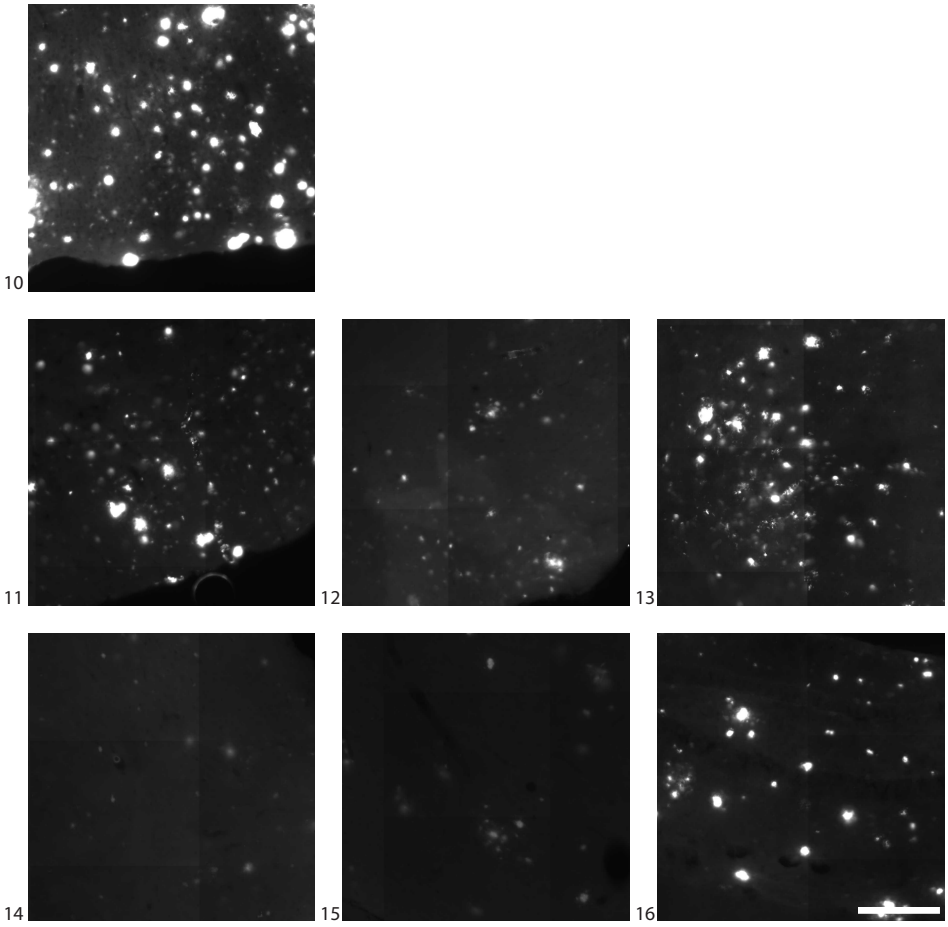

Figure 11.7 *In vivo* amyloid labeling
Shown are thirty micrometer brain sections of APP/PS1 transgenic mice resected injected with compound **10 – 16**. None of the wild type mice showed amyloid plaques or aspecific labeling. Scale bar = 200 µm

Summary and Conclusion

Several bis-pyridylethenylbenzenes have been prepared and evaluated for their Aβ binding properties and ability to pass the BBB. In general, all compounds showed affinity towards both human and murine fibrillar amyloid. Independent of the position of the nitrogen atom, the bis-pyridylethenylbenzenes without any additional groups seemed to show a higher affinity to amyloid in comparison with Methoxy-X04 (**10**). Besides the possible influence of the nitrogen atom, this might be due to their planar structure, which was previously suggested to be advantageous for a similar (bis)styrylbenzene with no further substituents.[20] The methoxy group on the inner ring structure seemed to result in a decrease in amyloid binding, particularly for human amyloid. However, in contrast to several known bis-styrylbenzenes, like **10**, the bis-pyridylethenylbenzenes did not share a common binding site with Chrysamine G.

In addition, all bis-pyridylethenylbenzenes seemed to cross the BBB and label amyloid *in vivo*. Based on the above results, compound **11**, (E,E)-1,4-bis(4-pyridylethenyl)benzene, showed the most favorable *ex* and *in vivo* characteristics and as such might serve as a starting point to further explore the potency of bis-pyridylethenylbenzenes.
A direct application of bis-pyridylethenylbenzenes for amyloid targeting would be their use in preclinical optical imaging. In addition we believe that the bis-pyridylethenylbenzene may serve as a novel backbone for the development of amyloid targeting PET or SPECT probes. As their binding sites may differ from existing amyloid targeting imaging probes, these compounds may provide additional information regarding accumulation of cerebral amyloid.

Materials and Methods

Preparation of $A\beta_{1-40}$ fibrils
Aβ fibrils were prepared by stirring a 0.5 mg/ml solution of $A\beta_{1-40}$ peptide (RPeptide, Bogart, GA) at 37 ºC for 3 days, which resulted in a cloudy solution. The presence of fibrils was confirmed by the presence of an emission peak at 482 nm (excitation 440 nm) upon addition of a 5 µM solution in PBS of Thioflavin T (Sigma, Germany) to a small amount of fibrils. Aliquots of 10 µl were transferred to Eppendorf vials and stored at -80 ºC until the assay was to be performed.

Fluorescence spectra
All compounds were dissolved in DMSO at 0.3 mM and diluted to 300 nM with 10 % ethanol in PBS (pH 7.2). Fluorescence spectra were measured on a Varian Cary Eclipse fluorescence spectrophotometer to obtain excitation and emission wavelength maxima, which were used to select the correct fluorescence filter settings for further microscopic evaluation. All measurements were carried out at 20 ºC and in triplicate. 3D emission-excitation spectra were obtained by adding 500 µl of the dissolved compounds to previously prepared Aβ aliquots. After manual shaking for 30 sec, 300 µl samples were measured (Infinity M1000, Tecan, Switzerland).

Staining of human and transgenic AD brain sections
Stock solutions of 3 mM in DMSO were diluted to 1 – 10 – 100 µM in 2:3 volume ratio PBS:ethanol and sonicated for 15 minutes. Paraffin sections (8 µm) of human AD cortex, 14 months old transgenic murine APP/PS1 brain and age-matched control cortices were deparaffinized prior to staining for 10 minutes in absolute darkness. After gently rinsing with tap water, sections were placed in 0.1 % NaOH in 80% ethanol for 2 minutes, air dried and coverslipped using Aqua / Polymount. Fluorescence of the stained sections was analyzed using a whole microscopic slide scanner (Pannoramic MIDI, 3DHistech, Hungary) with a DAPI filter cube (Ex 365 nm; Em 445/50 nm) using the same intensity setting throughout all experiments.

***In vivo* Aβ plaque labeling in transgenic AD mice**
Twelve-to-fourteen-month-old APP/PS1 mice or age-matched wildtype animals (n=2 per compound) were injected intravenously with 0.05 M dissolved in 1:1 volume ratio

DMSO:Cremophor diluted with PBS (pH 7.2) to a total volume of 200 µl, resulting in a total dose of 30 µmol/kg. One day after injection, animals were sacrificed using 200 µl Euthanasol (AST Pharma) prior to transcardial perfusion with 4% paraformaldehyde in PBS (pH 7.2). Brains were removed and cryoprotected in 4% PFA with 10% sucrose for 4 hours, followed by immersion in 4% PFA with 30% sucrose overnight. Snap-frozen brains were cryosectioned (30 µm) and fluorescence images were analyzed as described above.

Brain homogenates

Male, control and transgenic APP/PS1 mice (11 months old) were killed by decapitation. The cortices were removed and homogenized using a DUALL tissue homogenizer (20 strokes, 2000 rpm), in a 20-fold excess (v/w) of ice-cold 0.25 M sucrose. Homogenates were isolated by centrifugation (40 min x 250,000 x g) in a refrigerated Beckman ultracentrifuge (rotor 60-Ti). The resulting pellet was suspended in 20 volumes of 150 mM Tris + 20 % ethanol buffer (pH 7.0) for competition binding experiments.

Competition binding assay

Competition binding experiments were conducted at room temperature, in a final volume of 1 ml assay buffer (150 mM Tris-HCl, 20% ethanol, pH 7.0). Compounds were dissolved as 3 mM stock solutions in DMSO, sonicated for 15 min, and used in a final concentration range of 30 µM to 30 pM. 10 µl of unlabeled test compounds was combined with 890 µl of assay buffer and 50 µl of 100 nM [^{3}H]Chrysamine G stock (specific activity 33.8 Ci/mmol). The mixture was sonicated for 10 min, and the assay was subsequently started by the addition of 50 µl synthetic $A\beta_{1\text{-}40}$ fibrils or by addition of 400 µl of the brain homogenate suspension . Nonspecific binding was determined in the presence of 1 µM of **10**. Incubations were terminated after 1 h via filtration through Whatman GF/B filters (pre-soaked in binding buffer), using a 48-well Brandel harvester. The filters were washed two times with 3 ml of ice-cold binding buffer (pH 7.0), and radioactivity was determined by liquid scintillation spectrometry in 5 ml of Optiphase-HiSafe 3, at an efficiency of 40 %.

K_i values were determined by nonlinear regression analysis using the equation: logEC50 = log[10^logK_i*(1+RadioligandNM/HotK_dNM)] where K_d = 200 nM, and radioligand = 5nM. (GraphPad Software Inc., San Diego, CA)

Procedure for LogP determinations

LogP determinations were performed using literature procedures.[23] The measurements were performed on a Jasco HPLC-system (detection simultaneously at 214 and 254 nm) coupled to a Perkin Elmer Sciex API 165 mass instrument with a custom-made Electrospray Interface (ESI). An analytical Gemini C_{18} column (Phenomenex, 50 x 4.60 mm, 3 micron) was used in combination with buffers A) phosphate buffer of pH = 7.0 (0.02 M Na_2HPO_4 adjusted to pH = 7.0 with phosphoric acid) and B) 0.25% octanol in methanol.

Of all compounds to be evaluated, stock solutions of 0.5 mg ml^{-1} were prepared in methanol. These stock solutions were then diluted with water, making sure that the volume percentage of water was such that the compounds did not precipitate (max 40% water). A 0.25 mg ml^{-1} solution of $NaNO_3$ in water was used as a non-retaining compound to determine the dead time

of the system. For calibration purposes known compounds were taken from the literature. (**Table 3**) Of these compounds, 0.25 mg ml-1 solutions in either 75% H_2O/MeOH or 50% H_2O/MeOH were made.

For each sample, a series of four isocratic runs was performed, (for instance 55, 60, 65, 70% B), and the retention times (from UV-detection at 214 nm) thus obtained were converted to the retention factor k' according to the formula $k' = (t_R-t_0)/t_0$, with t_R being the retention time of the compound and t_0 being the retention time of $NaNO_3$. The retention factors were extrapolated to 0% B, yielding k'_w. As there is a linear relationship between LogP and log k'_w plotting LogP values of known compounds against obtained log k'_w values in this system yields a calibration curve. From this curve, LogP values of unknown compounds were calculated from their k'_w values.

Synthesis Procedures

General

Reagents and solvents were used as provided, unless stated otherwise. 2-pyridinecarboxaldehyde (**21**) and 4-pyridinecarboxaldehyde (**19**) were purchased from Acros, 3-pyridinecarboxaldehyde (**20**) was purchased from Sigma-Aldrich. THF was distilled over $LiAlH_4$ prior to use. Reactions were carried out under inert conditions and ambient temperature, unless stated otherwise. Prior to performing a reaction, traces of water were removed from the starting materials by repeated co-evaporation with anhydrous 1,4-dioxane or anhydrous toluene. These solvents were stored over 4 Å molsieves. Reactions were monitored by thin layer chromatography on aluminum coated silica sheets (Merck, silica 60 F254), using visualization either with iodine, or spraying with a solution of 25 g $(NH_4)_2MoO_4$, 10 g $(NH_4)_4Ce(SO_4)_4$ in 100 ml H_2SO_4 and 900 ml H_2O, or a solution of 20% H_2SO_4 in ethanol, followed by charring at ~150°C. Column chromatography was carried out with silica gel (Screening Devices bv, 40-63 µm particle size, 60 Å), using technical grade solvents. NMR spectra were recorded at 298K on a Bruker AV400 using deuterated solvents. All carbon spectra are proton-decoupled. Chemical shifts (δ) are given in ppm, in ^{13}C spectra relative to the solvent peaks of $CDCl_3$ (77.0 ppm) or CD_3OD (49.0 ppm), in ^{1}H spectra relative to the solvent peak of tetramethylsilane (0.0 ppm) or CD_3OD (3.31 ppm). Coupling constants are given in Hz. LC-MS analysis was performed on a Finnigan Surveyor

Table 11.3 Reference LogP values

Compound	LogP
Resorcinol	0.8
p-nitroaniline	1.39
Phenol	1.46
m-nitrophenol	2
2-naphtol	2.7
Naphthalene	3.37

Based on known literature values, the LogP of several reference compounds yield a required calibration curve to determine the LogP values of our compounds.[23-25]

HPLC system with a Gemini C_{18} 50 × 4.6 mm column (3 micron, Phenomenex, Torrance, CA, USA) (detection at 200-600 nm), coupled to a Thermo Finnigan LCQ Advantage Max mass spectrometer (Breda, The Netherlands) with electrospray ionization (ESI; system 1), with as eluents A: H_2O; B: MeCN and C: 1% aq. TFA. For RP-HPLC purification of the peptides, a Gilson GX-281 automated HPLC system (Gilson), supplied with a preparative Gemini C_{18} column (Phenomenex, 150 x 21.2 mm, 5 micron) was used. The applied buffers were A: 0.2% aq. TFA or 20 mM NH_4OAc and B: MeOH.
IR spectra were recorded on a Perkin Elmer Paragon 1000 FT-IR Spectrometer. High resolution mass spectra were recorded by direct injection (2 µL of a 2 µM solution in H_2O/MeCN; 50/50; v/v and 0.1% formic acid) on a mass spectrometer (Thermo Finnigan LTQ Orbitrap) equipped with an electrospray ion source in positive mode (source voltage 3.5 kV, sheath gas flow 10, capillary temperature 250 °C) with resolution R = 60000 at m/z 400 (mass range m/z = 150-2000) and dioctylpthalate (m/z = 391.28428) as a "lock mass". The high resolution mass spectrometer was calibrated prior to measurements with a calibration mixture (Thermo Finnigan). It should be noted that we did not obtain the suited HRMS data for every compound. This finding is in agreement with related compounds as reported earlier by us.. Based on the other characterization data obtained for each compounds we know for sure that our compounds are sound. For clarity, we here include the HMRS data that we did find: compound **14**: Exact mass: Calculated for $[C_{21}H_{19}N_2O]^+$: 315.14919. Found: 315.14901 $[M + H]^+$. compound **15** Exact mass: Calculated for $[C_{21}H_{19}N_2O]^+$: 315.14919. Found: 315.14915 $[M + H]^+$.

General procedure for the Horner-Wadsworth-Emmons reaction
The diphosphonate (0.95 mmol) was dissolved in THF (20 mL) and cooled to -10º C. KOtBu (0.30 g, 2.45 mmol) was added and the black mixture stirred for 20 min. A solution of the aldehyde (2.37 mmol) in THF (6 mL) was added and the reaction stirred at rt for 16 h. The reaction was cooled to 0ºC, quenched with water and extracted five times with EtOAc. The combined organic layers were dried (Na_2SO_4), filtered and concentrated. The crude product was subjected to column chromatography to yield the pure product.

(*E,E*)-1,4-bis(4-pyridylethenyl)benzene (11)
According to the general procedure, diphosphonate **17** (0.19 g, 0.5 mmol) was reacted with 4-pyridinecarboxaldehyde **19** (0.12 mL, 1.25 mmol). After work-up, the resulting yellow solids were purified by column chromatography (50 → 70% EtOAc/light petroleum) and the pure compound was obtained as a bright yellow solid (43 mg, 0.15 mmol, 30%).
^{1}H NMR ($CDCl_3$, 400 MHz): δ 8.59 (d, *J* = 5.6 Hz, 4H); 7.56 (s, 4H); 7.38 (d, *J* = 5.7 Hz, 4H); 7.30 (d, *J* = 16.3 Hz, 2H); 7.05 (d, *J* = 16.3 Hz, 2H). ^{13}C NMR ($CDCl_3$, 100 MHz): δ 150.1; 144.4; 136.5; 132.4; 127.5; 126.4; 120.8. IR (neat): 3442.0; 1591.6; 1414.1; 1217.5; 1118.9; 973.4; 868.4; 830.6; 595.9; 556.2. LC-MS retention time: 3.86 min (10 → 90% MeCN, 15 min run). Mass (ESI): *m/z* 285.13 $[M + H]^+$.

(*E,E*)-1,4-bis(3-pyridylethenyl)benzene (12)
According to the general procedure, diphosphonate **17** (0.19 g, 0.5 mmol) was reacted with 3-pyridinecarboxaldehyde **19** (0.12 mL, 1.25 mmol). After work-up, the resulting yellow solids

were purified by column chromatography (50 → 100% EtOAc/light petroleum) and the pure compound was obtained as a bright yellow solid (64 mg, 0.23 mmol, 45%).
^{1}H NMR ($CDCl_3$, 400 MHz): δ 8.73 (s, 2H); 8.49 (d, *J* = 4.3 Hz, 2H); 7.83 (d, *J* = 8.0 Hz, 2H); 7.53 (s, 4H); 7.29 (dd, *J* = 8.2 Hz, *J* = 5.1 Hz, 2H); 7.16 (d, *J* = 16.4 Hz, 2H); 7.09 (d, *J* = 16.4 Hz, 2H). ^{13}C NMR ($CDCl_3$, 100 MHz): δ 148.5; 148.5; 136.5; 132.9; 132.6; 130.1; 127.0; 125.0; 123.5. IR (neat): 3029.1; 1564.9; 1481.0; 1427.6; 1022.1; 965.9; 823.5; 704.8; 551.7. LC-MS retention time: 3.87 min (10 → 90% MeCN, 15 min run). Mass (ESI): *m/z* 285.13 $[M + H]^+$.

(*E,E*)-1,4-bis(2-pyridylethenyl)benzene (13)
According to the general procedure, diphosphonate **17** (0.19 g, 0.5 mmol) was reacted with 2-pyridinecarboxaldehyde **21** (0.12 mL, 1.25 mmol). After work-up, the resulting yellow solids were purified by column chromatography (0 → 20% EtOAc/light petroleum) and the pure compound was obtained as a bright yellow solid (20 mg, 0.07 mmol, 14%).
^{1}H NMR ($CDCl_3$, 400 MHz): δ 8.62 (d, *J* = 4.4 Hz, 2H); 7.70-7.64 (m, 2H); 7.65 (d, *J* = 16.2 Hz, 2H); 7.60 (s, 4H); 7.40 (d, *J* = 7.8 Hz, 2H); 7.20 (d, *J* = 16.0 Hz, 2H); 7.16 (dd, *J* = 7.0 Hz, *J* = 5.4 Hz, 2H). ^{13}C NMR ($CDCl_3$, 100 MHz): δ 155.5; 149.6; 136.7; 136.6; 132.2; 128.0; 127.5; 122.2; 122.1. IR (neat): 1634.1; 1581.5; 1559.8; 1467.9; 1431.7; 1333.4; 1205.7; 1145.3; 981.8; 873.8; 829.9; 763.9; 736.2; 609.6; 547.6. LC-MS retention time: 3.84 min (10 → 90% MeCN, 15 min run). Mass (ESI): *m/z* 285.13 $[M + H]^+$.

(*E,E*)-1-methoxy-2,5-bis(4-pyridylethenyl)benzene (14)
According to the general procedure, diphosphonate **18** (0.20 g, 0.5 mmol) was reacted with 4-pyridinecarboxaldehyde **19** (0.12 mL, 1.25 mmol). After work-up, the resulting yellow solids were purified by column chromatography (50% EtOAc/light petroleum → 2% MeOH/EtOAc) and the pure compound was obtained as a bright yellow solid (20 mg, 0.07 mmol, 14%).
^{1}H NMR ($CDCl_3$, 400 MHz): δ 8.60-8.55 (m, 4H); 7.80 (s, ^{1}H); 7.64 (d, *J* = 16.3 Hz, ^{1}H); 7.61 (d, *J* = 8.1 Hz, ^{1}H); 7.42 (d, *J* = 6.1 Hz, 2H); 7.40-7.36 (m, 4H); 7.17 (s, ^{1}H); 6.97 (d, *J* = 16.2 Hz, ^{1}H); 3.98 (s, ^{3}H). ^{13}C NMR ($CDCl_3$, 100 MHz): δ 156.5; 137.7; 131.7; 130.9; 128.7; 127.7; 127.3; 125.8; 120.9; 120.8; 119.9; 108.8; 55.9. IR (neat): 1633.9; 1590.5; 1463.7; 1417.6; 1389.6; 1323.3; 1297.7; 1116.6; 1029.2; 971.4; 819.7; 805.4; 616.0; 582.4; 548.1; 518.4. LC-MS retention time: 4.14 min (10 → 90% MeCN, 15 min run). Mass (ESI): *m/z* 315.2 $[M + H]^+$.

(*E,E*)-1-methoxy-2,5-bis(3-pyridylethenyl)benzene (15)
According to the general procedure, diphosphonate **18** (0.20 g, 0.5 mmol) was reacted with 3-pyridinecarboxaldehyde **20** (0.12 mL, 1.25 mmol). After work-up, the resulting yellow solids were purified by column chromatography (50% → 100% EtOAc/light petroleum) and the pure compound was obtained as a bright yellow solid (54 mg, 0.17 mmol, 34%).
^{1}H NMR ($CDCl_3$, 400 MHz): δ 8.79-8.65 (m, 2H); 8.48 (dd, *J* = 9.3 Hz, *J* = 4.7 Hz, 2H); 7.88-7.81 (m, 2H); 7.59 (d, *J* = 8.0 Hz, ^{1}H); 7.52 (d, *J* = 16.6 Hz, ^{1}H); 7.31-7.25 (m, 2H); 7.19-7.03 (m, 4H); 3.97 (s, ^{3}H). ^{13}C NMR ($CDCl_3$, 100 MHz): δ 157.3; 148.6; 148.5; 148.3; 137.7; 133.6; 132.8; 132.6; 132.6; 130.5; 126.9; 125.9; 125.4; 125.2; 125.1; 123.5; 123.5; 119.5; 115.6; 108.9; 55.6. IR (neat): 1633.7; 1567.2; 1557.6; 1479.8; 1463.5; 1423.3; 1328.1; 1240.6; 1164.2; 1117.7; 1035.0; 1024.0; 964.2; 819.8; 799.3; 705.5; 643.8; 627.1; 549.8.

LC-MS retention time: 4.14 min (10 → 90% MeCN, 15 min run). Mass (ESI): *m/z* 315.2 $[M + H]^+$.

(*E,E*)-1-methoxy-2,5-bis(3-pyridylethenyl)benzene (16)

According to the general procedure, diphosphonate **18** (0.20 g, 0.5 mmol) was reacted with 2-pyridinecarboxaldehyde **21** (0.12 mL, 1.25 mmol). After work-up, the resulting yellow solids were purified by column chromatography (0% → 30% EtOAc/light petroleum) and the pure compound was obtained as a bright yellow solid (42 mg, 0.13 mmol, 27%).

^{1}H NMR ($CDCl_3$, 400 MHz): δ 8.61 (s, 2H); 7.93 (d, *J* = 16.3 Hz, ^{1}H); 7.70-7.58 (m, 4H); 7.45 (d, *J* = 8.2 Hz, ^{1}H); 7.41 (d, *J* = 7.9 Hz, ^{1}H); 7.31-7.08 (m, 6H); 3.95 (s, ^{3}H). ^{13}C NMR ($CDCl_3$, 100 MHz): δ 157.6; 156.2; 155.5; 149.7; 149.5; 137.9; 136.6; 136.4; 132.4; 128.8; 128.2; 127.5; 127.4; 125.9; 122.1; 122.1; 121.8; 121.8; 119.9; 109.2; 55.5. IR (neat): 1584.0; 1562.5; 1467.9; 1430.5; 1248.3; 1036.0; 970.7; 769.3; 668.0. LC-MS retention time: 4.10 min (10 → 90% MeCN, 15 min run). Mass (ESI): *m/z* 315.07 $[M + H]^+$.

Tetraethyl 1,4-xylylene diphosphonate (17)

As described previously by Kikuchi *et al*.[26], a solution of $NaBrO_3$ (12.1 g, 80 mmol) in H_2O (40 mL) was added to a solution of p-xylene (2.47 mL, 20 mmol) in EtOAc (40 mL) and the mixture was vigorously stirred. A solution of $NaHSO_3$ (8.3 g, 80 mmol) in H_2O (80 mL) was added dropwise within 15 min and the reaction was stirred for 5 h. After the reaction mixture was poured out in Et_2O (300 mL), the layers were separated and the aqueous layer extracted twice with Et_2O. The combined organic layers were washed with 2 M $Na_2S_2O_3$, dried (Na_2SO_4), filtered and concentrated. The resulting white solids were subjected to column chromatography (0 → 5% EtOAc/light petroleum) and the product was obtained as a white solid (5.4 g), but not completely pure.

^{1}H NMR ($CDCl_3$, 400 MHz) δ 7.37 (s, 4H); 4.47 (s, 4H). ^{13}C NMR ($CDCl_3$, 100 MHz) δ 129.5; 32.8.

The impure 1,4-di(bromomethyl)benzene (5.4 g) was dissolved in triethyl phosphite (8.6 mL, 50 mmol) and the mixture was heated to reflux for 16 h. After cooling, the crude product was applied to a silica column and purified (50% EtOAc/light petroleum → 2% MeOH/EtOAc). The pure product was obtained as white fluffy powder (5.6 g, 14.8 mmol, 74% over two steps).

^{1}H NMR ($CDCl_3$, 400 MHz) δ 7.25 (s, 4H); 4.07-3.95 (m, 8H); 3.13 (d, *J* = 20.2 Hz, 4H); 1.24 (t, *J* = 7.1 Hz, 12H). ^{13}C NMR ($CDCl_3$, 100 MHz) δ 130.2; 130.1; 130.1; 129.9; 129.8; 129.7; 62.0; 62.0; 61.9; 34.0; 33.0; 16.3; 16.3; 16.2. ^{31}P NMR ($CDCl_3$, 162 MHz): δ 26.7 (s).

Tetraethyl 2-methoxy-1,4-xylylene diphosphonate (18)

As described previously by Kumar *et al*.[27], 2,5-dimethylanisole (1.36 g, 10 mmol) was dissolved in CCl_4 (22 mL). N-bromosuccinimide (3.92 g, 22 mmol) and benzoyl peroxide (20 mg) were added and the mixture heated to reflux for 2 h. After cooling to rt, the reaction mixture was filtered over Celite and concentrated. The resulting solids were purified by column chromatography (0 → 5% EtOAc/light petroleum). The dibromide was obtained as white solid (1.71 g, 5.8 mmol, 58%).

^{1}H NMR ($CDCl_3$, 400 MHz): δ 7.27 (d, *J* = 7.7 Hz, ^{1}H); 6.92 (dd, *J* = 7.6 Hz, *J* = 1.2 Hz, ^{1}H); 6.89 (s, ^{1}H); 4.52 (s, 2H); 4.44 (s, 2H); 3.88 (s, ^{3}H). ^{13}C NMR ($CDCl_3$, 100 MHz): δ 157.4; 139.7; 131.0; 126.3; 121.1; 111.5; 55.6; 33.2; 28.3.

Next, the 2,5-di(bromomethyl)-methoxybenzene (1.71 g, 5.8 mmol) was dissolved in triethyl phosphite (2.5 mL, 14.5 mmol) and the mixture was heated to reflux for 16 h. The mixture was

cooled, and directly applied to a silica column (50% EtOAc/PE → 4% MeOH/EtOAc). The pure product was obtained as a yellowish solid (1.55 g, 3.8 mmol, 66%).
^{1}H NMR ($CDCl_3$, 400 MHz): δ 7.25 (dd, *J* = 7.6 Hz, *J* = 2.9 Hz, ^{1}H); 6.86 (s, ^{1}H); 6.83 (d, *J* = 7.6 Hz, ^{1}H); 4.07-3.95 (m, 8H); 3.84 (s, ^{1}H); 3.21 (d, *J* = 21.4 Hz, 2H); 3.13 (d, *J* = 22.2 Hz, 2H); 1.27-1.20 (m, 12H). ^{13}C NMR ($CDCl_3$, 100 MHz): δ 157.2; 131.5; 131.1; 121.9; 121.900; 118.85; 112.1; 55.5; 34.4; 33.0; 27.0; 25.6; 16.3. 31P NMR ($CDCl_3$, 162 MHz): δ 27.39 (d, *J* = 9.0 Hz), 26.77 (d, *J* = 9.1 Hz).

References

1. Frisoni, GB, Fox, NC, Jack, CR, Jr., *et al*. The clinical use of structural MRI in Alzheimer disease. Nat Rev Neurol. 2010; 6:67-77.
2. Jack, CR, Jr., Knopman, DS, Jagust, WJ, *et al*. Hypothetical model of dynamic biomarkers of the Alzheimer's pathological cascade. Lancet Neurol. 2010; 9:119-128.
3. Vandenberghe, R, Van, LK, Ivanoiu, A, *et al*. ^{18}F-flutemetamol amyloid imaging in Alzheimer disease and mild cognitive impairment: a phase 2 trial. Ann Neurol. 2010; 68:319-329.
4. Barthel, H, Gertz, HJ, Dresel, S, *et al*. Cerebral amyloid-beta PET with florbetaben (^{18}F) in patients with Alzheimer's disease and healthy controls: a multicentre phase 2 diagnostic study. Lancet Neurol. 2011; 10:424-435.
5. GE beta-amyloid agent approved. J Nucl Med. 2013; 54:10N.
6. Yang, L, Rieves, D, and Ganley, C. Brain amyloid imaging--FDA approval of florbetapir F18 injection. N Engl J Med. 2012; 367:885-887.
7. Buell, AK, Esbjorner, EK, Riss, PJ, *et al*. Probing small molecule binding to amyloid fibrils. Phys Chem Chem Phys. 2011; 13:20044-20052.
8. Nesterov, EE, Skoch, J, Hyman, BT, *et al*. *In vivo* optical imaging of amyloid aggregates in brain: design of fluorescent markers. Angew Chem Int Ed Engl. 2005; 44:5452-5456.
9. Styren, SD, Hamilton, RL, Styren, GC, *et al*. X-34, a fluorescent derivative of Congo red: a novel histochemical stain for Alzheimer's disease pathology. J Histochem Cytochem. 2000; 48:1223-1232.
10. Kung, MP, Hou, C, Zhuang, ZP, *et al*. IMPY: an improved thioflavin-T derivative for *in vivo* labeling of beta-amyloid plaques. Brain Res. 2002; 956:202-210.
11. Klunk, WE, Bacskai, BJ, Mathis, CA, *et al*. Imaging Abeta plaques in living transgenic mice with multiphoton microscopy and methoxy-X04, a systemically administered Congo red derivative. J Neuropathol Exp Neurol. 2002; 61:797-805.
12. Higuchi, M, Iwata, N, Matsuba, Y, *et al*. ^{19}F and ^{1}H MRI detection of amyloid beta plaques *in vivo*. Nat Neurosci. 2005; 8:527-533.
13. Flaherty, DP, Walsh, SM, Kiyota, T, *et al*. Polyfluorinated bis-styrylbenzene beta-amyloid plaque binding ligands. J Med Chem. 2007; 50:4986-4992.
14. Nabuurs, RJA, Kapourchan, VV, Metaxas, A, *et al*. Polyfluorinated bis-styrylbenzenes as amyloid-beta plaque binding ligands. Bioorg Med Chem. 2014.
15. Bacskai, BJ, Hickey, GA, Skoch, J, *et al*. Four-dimensional multiphoton imaging of brain entry, amyloid binding, and clearance of an amyloid-beta ligand in transgenic mice. Proc Natl Acad Sci U S A. 2003; 100:12462-12467.
16. Bolander, A, Kieser, D, Scholz, C, *et al*. Synthesis of Methoxy-X04 Derivatives and Their Evaluation in Alzheimer's Disease Pathology. Neurodegener Dis. 2013.
17. Saroja, G, Soujanya, T, Ramachandram, B, *et al*. 4-Aminophthalimide derivatives as environment-sensitive probes. Journal of Fluorescence. 1998; 8:405-410.
18. Raymond, SB, Skoch, J, Hills, ID, *et al*. Smart optical probes for near-infrared fluorescence imaging of Alzheimer's disease pathology. Eur J Nucl Med Mol Imaging. 2008; 35 Suppl 1:S93-S98.
19. Ran, C, Xu, X, Raymond, SB, *et al*. Design, synthesis, and testing of difluoroboron-derivatized curcumins as near-infrared probes for *in vivo* detection of amyloid-beta deposits. J Am Chem Soc. 2009; 131:15257-15261.
20. Flaherty, DP, Kiyota, T, Dong, Y, *et al*. Phenolic bis-styrylbenzenes as beta-amyloid binding ligands and free radical scavengers. J Med Chem. 2010; 53:7992-7999.
21. Meadowcroft, MD, Connor, JR, Smith, MB, *et al*. MRI and histological analysis of beta-amyloid plaques in both human Alzheimer's disease and APP/PS1 transgenic mice. J Magn Reson Imaging. 2009; 29:997-1007.
22. Pike, VW. PET radiotracers: crossing the blood-brain barrier and surviving metabolism. Trends Pharmacol Sci. 2009; 30:431-440.
23. Benhaim, D and Grushka, E. Effect of n-octanol in the mobile phase on lipophilicity determination by reversed-phase high-performance liquid chromatography on a modified silica column. J Chromatogr A. 2008; 1209:111-119.
24. Lombardo, F, Shalaeva, MY, Tupper, KA, *et al*. ELogPoct: a tool for lipophilicity determination in drug discovery. J Med Chem. 2000; 43:2922-2928.
25. Lombardo, F, Shalaeva, MY, Tupper, KA, *et al*. ElogD(oct): a tool for lipophilicity determination in drug discovery. 2. Basic and neutral compounds. J Med Chem. 2001; 44:2490-2497.
26. Kikuchi, D, Sakaguchi, S, and Ishii, Y. An Alternative Method for the Selective Bromination of Alkylbenzenes Using NaBrO(3)/NaHSO(3) Reagent. J Org Chem. 1998; 63:6023-6026.

27. Kumar, P, Zheng, W, McQuarrie, SA, *et al*. ^{18}F-FESB: Synthesis and automated radiofluorination of a novel ^{18}F-labelled PET tracer for beta-amyloid plaques. J Labelled Comp Radiopharm. 2005;983-996.
28. Cohen, AD, Ikonomovic, MD, Abrahamson, EE, *et al*. Anti-Amyloid Effects of Small Molecule Abeta-Binding Agents in PS1/APP Mice. Lett Drug Des Discov. 2009; 6:437.